

## Influence of the bias current distribution on the static and dynamic properties of long Josephson junctions

M. R. Samuelsen and S. A. Vasenko

Citation: [Journal of Applied Physics](#) **57**, 110 (1985); doi: 10.1063/1.335383

View online: <http://dx.doi.org/10.1063/1.335383>

View Table of Contents: <http://scitation.aip.org/content/aip/journal/jap/57/1?ver=pdfcov>

Published by the [AIP Publishing](#)

---

### Articles you may be interested in

[Static vortices in long Josephson junctions of exponentially varying width](#)

Low Temp. Phys. **30**, 456 (2004); 10.1063/1.1768336

[Radio-frequency properties of stacked long Josephson junctions with nonuniform bias current distribution](#)

J. Appl. Phys. **85**, 6904 (1999); 10.1063/1.370210

[Static properties and current steps in one-dimensional parallel arrays of Josephson tunnel junctions in the presence of a magnetic field](#)

J. Appl. Phys. **79**, 322 (1996); 10.1063/1.360833


[Influence of the idle region on the dynamic properties of window Josephson tunnel junctions](#)

J. Appl. Phys. **77**, 2073 (1995); 10.1063/1.358848

[Critical Currents and Current Distributions in Josephson Junctions](#)

J. Appl. Phys. **40**, 1813 (1969); 10.1063/1.1657852

---


The Shimadzu logo, consisting of a stylized 'S' inside a circle, is positioned to the left of the company name.**SHIMADZU**  
Excellence in Science

**Powerful, Multi-functional UV-Vis-NIR and FTIR Spectrophotometers**

Providing the utmost in sensitivity, accuracy and resolution for applications in materials characterization and nano research

- Photovoltaics
- Polymers
- Thin films
- Paints
- Ceramics
- DNA film structures
- Coatings
- Packaging materials

[Click here to learn more](#)

A row of four Shimadzu spectrophotometers is shown. From left to right: a small, compact model; a medium-sized model with a sample compartment; a larger, more complex model with multiple compartments; and a tall, vertical model with a large sample area.

# Influence of the bias current distribution on the static and dynamic properties of long Josephson junctions

M. R. Samuelsen<sup>a)</sup> and S. A. Vasenko

Department of Physics, Moscow State University, Moscow 119899 GSP, USSR

(Received 23 April 1984; accepted for publication 20 June 1984)

The maximum supercurrent through a long and narrow Josephson junction has been calculated numerically as a function of an applied magnetic field for various feed current distributions. The results have been shown to depend drastically on the mode of the current feed. In particular, the real nonuniform distribution  $\eta_{ov}(x)$  of the current corresponding to the overlap geometry of the junction is nearly equivalent to the mixture  $y\eta_{un} + (1-y)\eta_{in}$  with the factor  $y$  approaching unity as the junction length increases:  $(1-y) = C_y(L/\lambda_J)^{-0.5}$ ,  $C_y \simeq 1.7$ . In contrast with the static properties, the shape of the zero-field step in the long junction  $I$ - $V$  curve appears to be almost independent of the mode of the current feed, because of averaging of the Lorentz force by the travelling Josephson vortices.

## I. INTRODUCTION

It is well known<sup>1-3</sup> that the mode of the current feed ("injection") into the Josephson junctions can affect their static and dynamic properties. For the overlap geometry, where the bias current is injected into the junction perpendicular to its long direction [see Fig. 1(a)], most theoretical treatments have assumed uniform distribution of the injected current along the junction length.<sup>3-5</sup> However, in the absence of the superconducting ground plane the current density distribution across the width of a superconducting electrode film<sup>6</sup> and, hence, the injected current distribution along the junction length are essentially nonuniform [see Fig. 1(b)]. This distribution has singularities at the junction edges making the situation close to a mixture of the uniform and edged current feed.<sup>3</sup>

The purpose of this work has been—for the first time—to find numerically the boundaries of the static state and the shape of the first zero-field step in  $I$ - $V$  curve of the overlap-type junction with this real (nonuniform) current junction injection important for the utilization of fluxon dynamics in real circuits and to compare these results with those for some other modes of the injection.

## II. MODEL

A long and narrow rectangular junction of length  $L$  and width  $W$  ( $L \gg \lambda_J \gg W$ ,  $\lambda_J$  being the Josephson penetration depth) may be described by the perturbed sine-Gordon equation

$$\phi_{xx} - \phi_{tt} = \sin \phi + \alpha \phi_t - \eta(x), \quad (1)$$

where we use the ordinary dimensionless units (see, e.g., Ref. 3). Equation (1) is virtually exact for a static state ( $\partial/\partial t = 0$ ) and may also be used as a reasonable approximation for the junction dynamics.<sup>2</sup> In this work we will consider the following distributions of the injected current density  $\eta(x)$ :

$$\eta_{un}(x) = \eta_0 \quad (\text{uniform}), \quad (2a)$$

$$\eta_{in}(x) = \eta_0 [\delta(x) + \delta(l-x)] \quad (\text{in-line}), \quad (2b)$$

$$\eta_{ov}(x) = (\eta_0 l / \pi) / \sqrt{x(l-x)} \quad (\text{overlap}). \quad (2c)$$

Here  $\eta_0$  is the mean linear current density in units of  $j_c W$ , where  $j_c$  is critical current density,  $l = L/\lambda_J$ . If an external magnetic field  $H$  is applied in the plane of the junction and perpendicular to its long direction, it imposes the following boundary conditions for Eq. (1):

$$\phi_x(0, t) = \phi_x(l, t) = \kappa \equiv H / j_c \lambda_J. \quad (3a)$$

Note that Eqs. (2b) and (3a) can be united as follows:

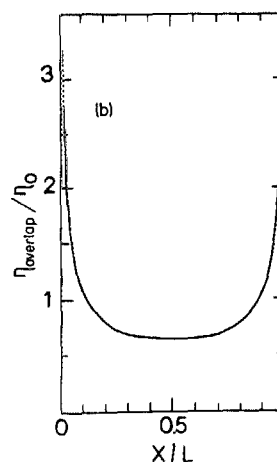
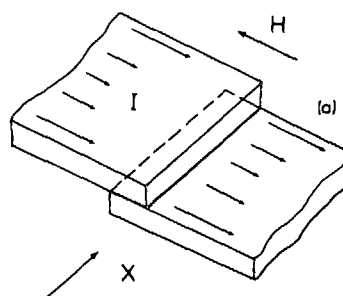


FIG. 1. The overlap Josephson junction. (a) Sketch of the junction geometry. (b) Distribution of the injected current along the junction length.

<sup>a)</sup>Permanent address: Physics Laboratory I, The Technical University of Denmark, DK-2800 Lyngby, Denmark.

$$\phi_x(0,t) = \kappa - \eta_0 l / 2, \quad \phi_x(l,t) = \kappa + \eta_0 l / 2. \quad (3b)$$

When solving Eq. (1) numerically with the boundary conditions (3) we have used a standard implicit finite-difference method with  $\Delta x = 0.1$  and  $\Delta t = 0.05$ . Such parameters have turned out to be sufficient for the accuracy of the results to be not worse (but often much better) than 1%. The distribution (2c) has been cut off at the boundary points in order to make the numerical integral of  $\eta_{ov}(x)$  equal to  $\eta_0 l$ .

### III. MAXIMUM SUPERCURRENT

In order to determine the maximum supercurrent  $\eta_0 l$  as a function of the external magnetic field  $\kappa$  we looked for a static solution of Eqs. (1) and (2c) starting usually with the initial conditions  $\phi(x,0) = \sin^{-1} \eta_0$  and  $\phi_t(x,0) = 0$ . After the time iterations had been started we have averaged the dimensionless voltage  $\phi_t$  over long (of the order of hundred time units) consequent time intervals and simultaneously over the junction length. If the mean voltage had become less than  $10^{-5}$  we believed that the static state had been reached. To be certain that no vortices have entered the junction we checked the difference  $\phi(l,t) - \phi(0,t)$  after each interval. Then we used the calculated phase distribution as a new initial condition for another run with some larger current value. The procedure was continued until we reached the boundary of the static solution. Then the adjustment of the current value had been performed to determine the boundary with the accuracy better than one per cent.

Figure 2 shows the critical current of the junction for various types of the current feed and for two junction lengths: (a)  $l = 10$  and (b)  $l = 20$ . One can see that the critical current value depends drastically on the mode of the current injection. The largest critical current always corresponds to the uniform current feed Eq. (2a) for which a simple result<sup>1</sup>

$$(\kappa/2)^2 = (1 - \eta_0^2)^{0.5} - \sin^{-1}(1 - \eta_0^2)^{0.5} \eta_0 \quad (4a)$$

holds true for  $l \gg 1$ . The lowest  $\eta_0$  takes place for the edge current injection Eq. 2(b); for  $l \gg 1$  the following simple formula is valid:

$$\eta_0 l / 2 + |\kappa| = 2, \quad (4b)$$

and, hence, the critical current decreases as  $l^{-1}$  with the increase of the junction length. According to Eq. (3b) this formula means that the critical state of the junction is reached when the smallest of the total currents  $I_t = I \pm HW$  injected at the junction edges reaches the critical value  $I_m = 2\lambda_J j_c$  (Ref. 7).

Finally, the critical current for the nonuniform distribution is always located between the value Eqs. (4a) and (4b).

It has been proposed<sup>3</sup> to approximate the real type of the current injection  $\eta_{ov}(x)$  by the following linear mixture:

$$\eta_{mix}(x) = y\eta_{un}(x) + (1 - y)\eta_{in}(x), \quad (5)$$

where the factor  $y$  shows the part of the whole current  $\eta_0 l$  being uniformly injected along the junction length. We have compared the  $\eta_0(\kappa)$  dependence for the distributions (2c) and (5) and have found a fair agreement (with an accuracy of the order of 1%) if the proper value of the factor  $y$  has been chosen. This value of factor  $y$  depends essentially on the junction length. For example,  $y = 0.72 \pm 0.01$ , for  $l = 10$

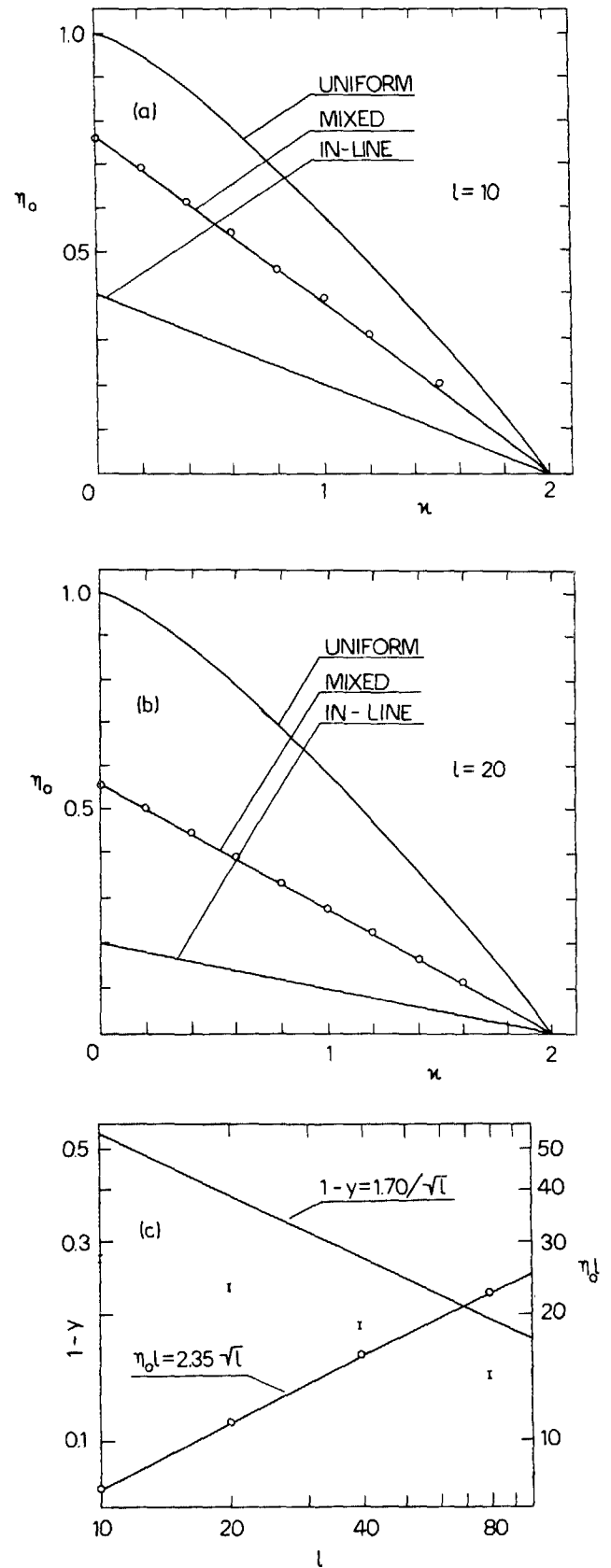


FIG. 2. The critical current  $\eta_0 l = I/I_c$  ( $I_c = j_c W \lambda_J$ ) as a function of the external magnetic field ( $\kappa \equiv H/j_c \lambda_J$ ) and the junction length ( $l = L/\lambda_J$ ). The points and the error bars (for the parameter  $1 - y$ ) represent the results of the numerical calculations for the real current injection (Eq. 2c) to the overlap junction. The errors result from the uncertainty of  $\eta_0$ . (a)  $l = 10$ , (b)  $l = 20$ , (c)  $\kappa = 0$ .

and  $y = 0.77 \pm 0.01$ , for  $l = 20$  [see Figs. 2(a) and 2(b)].

It is easy to explain this dependence for the case of the long junctions ( $l \gg 1$ ). For such junctions the critical current in the range  $|\kappa| < 2$  corresponds to nucleation of the first Josephson vortex at the junction edge ( $x = 0$  or  $x = l$ ). This process is localized at the distance of the order of  $\lambda_J$  near the junction edge and hence only the injected current distribution near the edge is of importance. For the nonuniform current density Eq. (2c) at  $x = 0$ ,  $\eta_{ov}(x) \approx (\eta_0/\pi) (l/x)^{0.5}$ . Thus at  $x = 0$ , our boundary problem has a single parameter  $\eta_0 l^{0.5}$  which shows that  $\eta_0$  scales as  $l^{-0.5}$  and that for the whole critical current we have

$$\eta_0 l = C_\eta l^{0.5}; \quad (6)$$

our numerical calculations show that  $C_\eta = 2.35 \pm 0.05$ . On the other hand, for the mixture in Eq. (5) the second term alone is important at  $l \rightarrow \infty$ , so that the critical current is given by the modified Eq. (4b):

$$(1 - y)\eta_0 l / 2 + \kappa = 2. \quad (4c)$$

Comparison of Eqs. (6) and (4c) yields:

$$\begin{aligned} 1 - y &= C_y(\kappa) l^{-0.5}, \\ C_y(\kappa) &= 2(2 - \kappa)/C_\eta, \\ C_y(0) &\approx 1.70. \end{aligned} \quad (7)$$

Figure 2(c) shows the  $\eta_0 l$  and  $(1 - y)$  on  $l$  dependences for  $\kappa = 0$ . The first is indeed very close to the asymptotic function given by Eq. (6), while the second one approaches the asymptotic value more slowly.

#### IV. FIRST ZERO-FIELD STEP

When the current exceeds its critical value, the first vortex enters the junction and moves along it being dragged by the Lorentz force applied by the injected current. This vortex motion results in the well-known current steps in the  $I$ - $V$  curve. When sweeping the junction (with low damping) to and fro, the vortex averages this Lorentz force. Thus, one may expect the vortex dynamic properties for  $\alpha \ll 1$  to be much less sensitive to the mode of the current injection than that of the static ones. To check it we have calculated the first zero-field step ( $\kappa = 0$ ) for the three modes of the current injection considered above.

The calculations started with the initial conditions  $\phi(x, 0) = \phi^s + \sin^{-1} \eta_0$  and  $\phi_t(x, 0) = \phi_t^s(x, 0)$ ,  $\phi^s$  being the soliton solution of the pure sin Gordon equation.<sup>8</sup> The proper soliton propagation velocity was found from the well-known energy balance equation.<sup>9</sup> To get the average voltage we used the same procedure as in static case but for the dynamic situation we compared the voltage values corresponding to the neighboring time intervals. When their difference became less than 0.1% the last of these values was accepted to be the true average voltage. Besides, we have used in contrast with the static case some larger averaging time intervals (for the lowest part of the step they reached a thousand dimensionless units of time). In order to move along the zero-field step we used the previous phase distribution as a new initial one to get the next numerical solution corresponding to a next current value.

Figure 3 shows the shape of the first current step for the

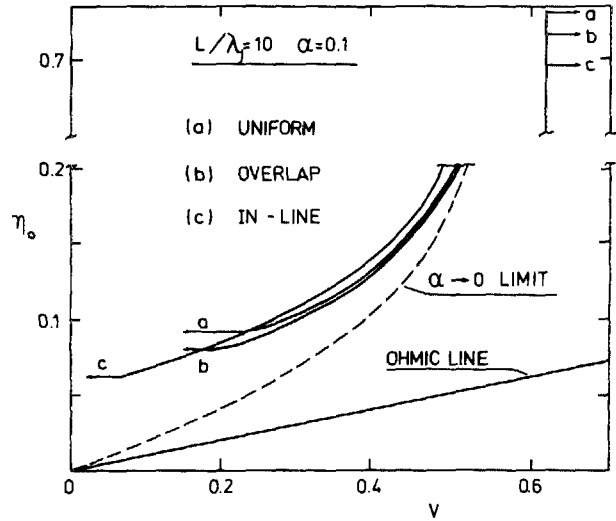


FIG. 3. The first zero-field step (numerically calculated) for various modes of the current feed. The dashed curve  $\{V = (2\pi/l)[1 + (4\alpha/\pi\eta_0)^2]^{-0.5}\}$  corresponds to the infinite junction with the dissipation parameter  $\alpha \rightarrow 0$ .<sup>9</sup>

uniform injection, the real  $\eta_{ov}(x)$  injection, and the in-line one. For comparison, the dashed line shows the universal theoretical curve value for any mode of the current injection in the limit  $\alpha \rightarrow 0$ . One can see from Fig. 3 that the dynamic properties of the junction are indeed much less dependent on the mode of the current feed than the static ones.

In conclusion, we have shown that a change of the modes of the current injection can result in the drastic changes of the static properties of the junction. In contrast, the dynamic properties of the junction are found to be much less dependent on the distribution of the injected current.

The mixed-injection approximation turns out to be a very good one for the overlap junction if the parameter  $y$  is chosen in a proper way (Fig. 2).

#### ACKNOWLEDGMENTS

We gratefully acknowledge useful conversations with K. K. Likharev, V. K. Semenov, and V. P. Zavaleev, and one of us (MRS) is grateful for the financial support from the Danish-Soviet cultural exchange program.

<sup>1</sup>M. Yu. Kuprijanov, K. K. Likharev, and V. K. Semenov, Sov. J. Low Temp. Phys. 2, 610 (1976) [Fiz. Nizk. Temp. 2, 1252 (1976)].

<sup>2</sup>N. F. Pederson and D. Welner, Phys. Rev. B 29, 2351 (1984).

<sup>3</sup>O. H. Olsen and M. R. Samuelsen, J. Appl. Phys. 54, 6522 (1983).

<sup>4</sup>O. A. Levring, N. F. Pedersen, and M. R. Samuelsen, J. Appl. Phys. 54, 987 (1983).

<sup>5</sup>O. H. Olsen and M. R. Samuelsen, Phys. Rev. B 28, 210 (1983).

<sup>6</sup>V. L. Newhouse, J. W. Bremer, and H. H. Edwards, Proc. IRE 48, 1395 (1960).

<sup>7</sup>C. S. Owen, and D. J. Scalapino, Phys. Rev. 164, 538 (1967).

<sup>8</sup>A. C. Scott, F. Y. F. Chu, and D. W. McLaughlin, Proc. IEEE 61, 1443 (1973).

<sup>9</sup>T. A. Fulton and R. C. Dynes, Solid State Commun. 12, 57 (1973).